DOI 10.1515/revac-2012-0043 — Rev Anal Chem 2013; 32(2): 91–101

Jing Wang and Heyou Han*

Near-infrared electrogenerated chemiluminescence from quantum dots

Abstract: Since the electrogenerated chemiluminescence (ECL) of silicon quantum dots (QDs) was reported in 2002, a series of QDs with different sizes, components, and shapes has been extensively studied as ECL emitters for biosensors. Lately, near-infrared (NIR) ECL analysis has emerged as an alternative to traditional visible-range ECL bioassays, especially in some complex biological systems. This is because the NIR spectral region could provide a "clear window" to effectively fulfill the requirement of interference-free sensing. Among the present reported ECL emitters, QDs hold great promise as NIR ECL emitters owing to their size or surface-dependent luminescence and photochemical stability. This review presents a general picture of the latest advances and developments related to QDs for NIR ECL emitters. It briefly covers the synthetic strategies of NIR QDs and the advances in QD-based NIR ECL and related biosensing methodologies. Finally, we conclude with a look at the future challenges and prospects in the development of QD-based NIR ECL.

Keywords: biosensor; electrogenerated chemiluminescence; near infrared; quantum dots; synthesis.

***Corresponding author: Heyou Han**, State Key Laboratory of Agricultural Microbiology, College of Science, Huazhong Agricultural University, Wuhan 430070, P.R. China, e-mail: hyhan@mail.hzau.edu.cn

Jing Wang: State Key Laboratory of Agricultural Microbiology, College of Science, Huazhong Agricultural University, Wuhan 430070, P.R. China

Introduction

Electrogenerated chemiluminescence (also known as electrochemiluminescence, or ECL) is an electrochemically triggered optical radiation process that involves the generation of species at electrode surfaces that then undergo electron-transfer reactions to form excited states, which eventually emit light (Miao 2008). Analogous to chemiluminescence, ECL does not require the use of external light sources. The smart combination of chemiluminescence and electrochemistry brings ECL many potential advantages such as rapidity, high sensitivity, simplified optical setup, and no background from unnecessary photoexcitation (Richter 2004, Hu and Xu 2010). To date, different luminescent reagents have been exploited in ECL behaviors, which mainly include organic systems (e.g., luminol) (Zhang et al. 2005), inorganic systems (e.g., metal complexes) (Zu and Bard 2000, Dennany et al. 2003, 2006), and nanoparticle systems (e.g., quantum dots, or QDs) (Ding et al. 2002, Myung et al. 2002, Bae et al. 2004). Among them, commercial ECL detection systems based on $Ru(bpy)_3^{2+}$/tri-*n*-propylamine (TPrA) (Miao et al. 2002, Zhan and Bard 2006) and luminol-H_2O_2 (Wilson et al. 2003, Tian et al. 2010) have been widely investigated in biomedical and diagnostics assays. Because finding new luminescence materials with a high ECL efficiency for bioanalysis is the constant driving force of this area, semiconductor nanocrystals (QDs) have attracted considerable attention as a new kind of ECL emitters since 2002 owing to their distinctive merits such as high fluorescence quantum yields, size or surface trap-controlled luminescence, and good stability against photobleaching (Ding et al. 2002). In recent years, various kinds of QD-based ECL emitters including II–VI, III–V, and IV–VI nanocrystals (Zou and Ju 2004, Han et al. 2007, Jie et al. 2007, Mokkapati and Jagadish 2009, Hu et al. 2010), carbon nanodots (Zheng et al. 2009, Baker and Baker 2010), and metallic nanoclusters (Díez et al. 2009, Li et al. 2011) have been used in fabricating ECL sensors, and several classical reviews concerning QD-based ECL systems have been published (Qi et al. 2009, Li et al. 2012, Deng and Ju 2013).

Although current ECL probes are popular tools in analytical research, most challenges arise with the increase in some complex samples such as living cells or biological fluids. This is because most of the emitting spectra of the above-mentioned ECL labels are mainly located in the visible ranges. It is worth mentioning that near-infrared (NIR) fluorescence has attracted much more interests in biomedical imaging and diagnostics applications because NIR emission offers several advantages, including minimal interferential absorption, low biological autofluorescence, and high tissue penetration (Frangioni 2003, Kim et al. 2003b). Similar to NIR fluorescence, the NIR ECL analysis technique could probably provide an alternative to the traditional ECL bioassays and give a new perspective toward

the ECL-based detection in complex biological samples. Thus, developing novel ECL probes with emission profiles at 700–900 nm is the key to circumvent those limitations. With the development of synthetic strategies of NIR QDs, great efforts have been made toward ECL studies from NIR QDs because of their promising NIR ECL property (Sun et al. 2009, Liang et al. 2010, Wang et al. 2011, Zou et al. 2011, Cui et al. 2012). Currently, the reported work mainly focused on the fundamental properties and theoretical explanations of NIR ECL from QDs; the rational design of biosensors based on NIR ECL from QDs remains unexplored totally until now (Liang et al. 2011b, 2012, Cui et al. 2012, Wang et al. 2012). Therefore, the disposable QD-based NIR ECL sensors and novel NIR ECL emitters are highly desired for practical applications of ECL detection.

The exploration and advancement concerning QD-based NIR ECL not only open a promising field for the development of new-generation ECL-emitting species but also complement the conventional optical utilizations of QDs as well. This article aims to provide a concise review covering various synthesis methods for NIR QDs. More attention is paid to the QD-based NIR ECL phenomenon and their sensing applications. Finally, we also discuss the NIR ECL limitations in the application fields.

Synthesis of NIR QDs

In recent years, there is an explosion of interest in creating NIR nanocrystals, imparting momentum to the development of the next-generation imaging probes and opening up new avenues in biomedical and biological studies (Cai et al. 2006, Allen et al. 2009, Choi et al. 2009, Xie and Peng 2009, Yong et al. 2009, Gao et al. 2010). The present strategies of synthesizing NIR QDs can be divided into two parts, including the use of narrow-band-gap materials and charge carrier separation by staggering band offsets (type II QDs) (Ma and Su 2010). In the following section, we will discuss these methods in detail.

Narrow-band-gap NIR QDs

To achieve the goal of NIR emission, one has to select suitable semiconductor materials with bulk band-gap energy lower than the NIR energy to prepare mononuclear or alloyed QDs (AQDs) by controlling their growth sizes or structure compositions, generally containing type III–V NIR QDs, type II/IV–VI NIR QDs, and alloyed NIR QDs (Ma and Su 2010).

The usually studied compounds of type III–V NIR QDs to date were focused on InP and InAs QDs because their emissions can be readily tuned throughout the visible and NIR ranges by changing their sizes. However, the organic phase synthetic procedure of type III–V NIR QDs is more difficult and complicated, and the as-prepared QDs always exhibit rather poor optical properties such as low emission efficiency, broad spectrum width, and poor size control and stability (Guzelian et al. 1996, Mićić et al. 1997). Recently, several methods including new procedures for core growth (Xie et al. 2007), epitaxial growth of shell materials on the cores (Mićić et al. 2000, Haubold et al. 2001), and posttreatments of initial synthetic products (Talapin et al. 2002) have been extensively exploited to push forward the development of type III–V NIR QDs. Li et al. (2008) reported a novel and economic approach for the preparation of InP cores based on the *in situ* generation of phosphine gas from a calcium phosphide precursor. Subsequent coating with a ZnS shell led to a photoluminescence quantum yield (PLQY) in the range of 10%–22%, depending on emission wavelength. Xie and Peng (2008) reported the synthesis of high-quality InAs QDs for NIR emission based on self-focusing. This new strategy also provided a suitable route for one-pot growth of core/shell nanocrystals with bright, stable, and narrow photoluminescence (PL) in the NIR window.

Although type II–VI QDs are the largest group of QDs, the number of type II–VI NIR QDs is far less than that of the type II–VI visible QDs, mainly including HgX (Te, S) (Higginson et al. 2002, Green et al. 2003) and CdTe QDs. CdTe QDs exhibiting a smaller bulk band gap than CdSe (1.5 vs. 1.75 eV at 300 K) is, in principle, a good candidate for the fabrication of NIR QDs (Reiss et al. 2009). Several synthetic ideas have been applied to tune the emission of CdTe QDs according to growth temperature control (Peng and Peng 2000), additional precursor injection (Talapin et al. 2001), or even chemical surface modification using different surfactants (Akamatsu et al. 2005). However, the shell materials for CdTe exhibit a large lattice mismatch, leading to a low PLQY in organic solvents. Therefore, the preparation of thiol-stabilized NIR CdTe QDs in aqueous media could be a better choice (Zou et al. 2008, Liang et al. 2011a). For example, He et al. (2011a) reported a facile one-step microwave-assisted method for directly synthesizing NIR CdTe QDs in aqueous phase with strong PLQY (15%–20%). Also, lead-based IV–VI QDs have attracted much more attention in the past as a kind of efficient NIR fluorophore. PbS and PbSe QDs have been successfully prepared through both organometallic and aqueous synthesis approaches (Hinds et al. 2007, Evans et al. 2008). The

PL and ECL from high-quality PbS QDs have been studied in the NIR wavelengths (Sun et al. 2009).

AQDs open new possibilities in band-gap engineering and in developing NIR nanoprobes (Bailey and Nie 2003). As an ideal candidate for application in NIR emission, some NIR AQDs were first synthesized in the organic phase by an organometallic method that restricted their direct applications in biosystems (Allen and Bawendi 2008, Xie and Peng 2009). Further, the phase-transfer process also produced some drawbacks, including decreased stability and fluorescence efficiency. Recently, several highly luminescent NIR AQDs have been directly prepared in aqueous solutions. For example, Mao et al. (2007) presented a facile one-pot hydrothermal method to fabricate water-dispersed NIR CdTeS AQDs with high PLQY. Zhu's group prepared high-quality NIR CdSeTe AQDs in an aqueous medium following a facile one-pot refluxing route (Liang et al. 2009). Upon ZnS shell growth under microwave conditions, a novel and efficient NIR ECL reagent was obtained (Liang et al. 2010).

The toxicity of QDs has attracted intense attention for their application *in vivo*. There are several low-toxicity QDs in the first or second NIR region, which mainly includes Ag_2Se (Gu et al. 2012, Zhu et al. 2013), Ag_2S (Du et al. 2010, Jiang et al. 2012), and Si QDs (Erogbogbo et al. 2008, He et al. 2011b). Although the synthetic technologies were less mature and the procedures were relatively complicated, much effort has been devoted to develop new methods for the preparation of these high-quality QDs. For instance, Pang's group has coupled Na_2SeO_3 reduction with the binding of silver ions and alanine to successfully realize the preparation of NIR emission-tunable, small, less cytotoxic, and water-dispersible Ag_2Se QDs (Gu et al. 2012). Wang and colleagues first reported the synthesis of NIR Ag_2S QDs *via* the pyrolysis of Ag(DDTC) in the organic phase, and the obtained QDs possessed good monodispersity, small size, and high PLQY (Du et al. 2010). Further, through the bioconjugation of Ag_2S QDs with specific ligands, these nanoprobes hold great promise for the targeted labeling and imaging of cells (Zhang et al. 2012).

Type II NIR QDs

The emission wavelength of type II QDs, with the valence band edge or the conduction band edge of the shell material located in the band gap of the core, could be tuned across the visible to the NIR regions by controlling the thickness of the shell or the core size (Reiss et al. 2009). Thus far, there are several type II NIR QD systems, such as CdTe/CdSe (Kim et al. 2003a), ZnTe/CdTe (CdSe, CdS) (Xie et al. 2005), and CdSe/ZnTe (Chen et al. 2004), and a series of high-quality type II core/shell NIR QDs has been successfully prepared in both organic and aqueous phases. It is noteworthy that the research on colloidal type II NIR QDs was triggered by the seminal work of Bawendi and colleagues (Kim et al. 2003a). In their work, CdTe/CdSe QDs emit at lower energies than CdTe, covering the spectral range from 700 to 1000 nm. This type of QDs could also be obtained directly from an aqueous medium. Yan and colleagues reported a layer-by-layer colloidal epitaxial growth of L-cysteine-capped CdTe/CdSe type II core/shell QDs in an aqueous solution with emissions between 600 and 850 nm (Zhang et al. 2009). Inspired by this, our group developed a hydrothermal technique for the NIR CdTe/CdSe QDs, wherein the PLQY was further improved to 40% in the aqueous phase (Wang and Han 2010).

Recently, the lattice mismatch strain tuning theory has emerged as a fascinating strategy to convert standard type I QDs into type II heterostructures, resulting in the red shift of the emission spectrum and, consequently, the NIR QDs (Smith et al. 2008). Nie described a class of wurtzite CdTe core based on core/shell nanocrystals that were converted into type II QDs by lattice strain in the organic phase; the strain induced by the lattice mismatch could be used to tune the light emission – which displayed a narrow line width and a high PLQY – across the visible to the NIR part of the spectrum (500–1050 nm) (Smith et al. 2008). Deng et al. (2010) reported a two-step low-temperature aqueous method based on the lattice mismatch strain between the CdTe core and the CdS shell materials for synthesizing water-soluble CdTe/CdS $core_{magic}/shell_{thick}$ QDs, whose NIR emission (475–810 nm) could be tuned by varying the shell thickness (Figure 1). Following this line of thought, our group used air-stable and commercial Na_2TeO_3 as Te source to replace traditional NaHTe or H_2Te and proposed a one-pot aqueous approach for producing highly luminescent NIR CdTe/CdS $core_{small}/shell_{thick}$ QDs with the PLQY up to 65% (Chen et al. 2012).

NIR QDs as NIR ECL emitters

Although a number QD-based ECL systems and even various kinds of synthesis routes for NIR QDs have been developed since 2002, the first comprehensive and systematic observation of the ECL phenomenon from NIR QDs was in 2009 (Sun et al. 2009). At present, there are only several QD-based NIR ECL emitters, and we categorize these nanoemitters into two parts by their compositions.

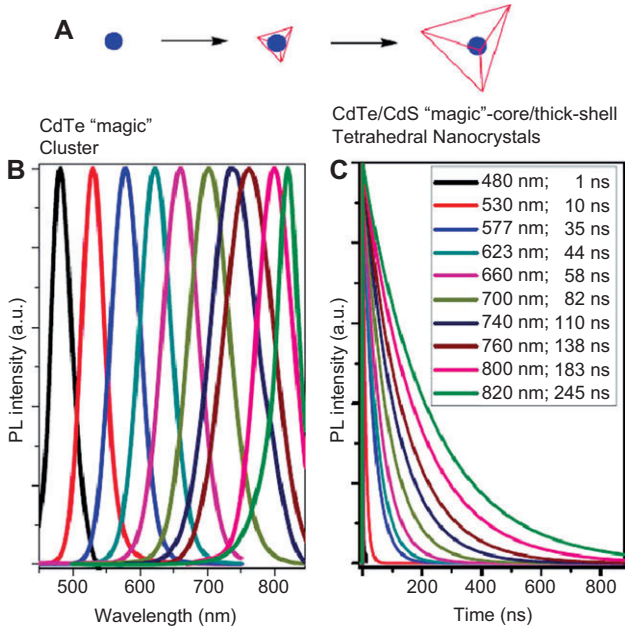

Figure 1 (A) Schematic diagram illustrating the formation of the CdTe/CdS magic-core/thick-shell tetrahedral NCs. (B) Room-temperature PL emission profiles of a series of NC samples obtained by varying the CdS shell growth to overcoat the magic-sized CdTe core with thicker shells. (C) Room-temperature PL decay kinetics monitored at the maximum emission wavelengths of the samples in (B). The calculated excited state lifetimes are listed. (Reproduced with permission from ACS Publication.)

Binary component QDs

PbS QDs are efficient NIR-emitting materials as their narrow band gap. Sun et al. (2009) first reported the NIR ECL property from PbS QDs in an organic electrolyte solution. The ECL emission of PbS QDs was realized through an annihilation course. During potential cycling, the conduction and the valence band of PbS QDs can accept (electron-injected) and donate (hole-injected) electrons to form reduced ($QD^{\bullet-}$) and oxidized ($QD^{\bullet+}$) QDs, respectively. The electron-transfer annihilation of two oppositely charged QDs resulted in the production of excited- and ground-state QDs; then, the excited QD returned to the ground state *via* a radiative pathway by emitting a photon, which was described as follows:

$$QD\text{-}e \rightarrow QD^{\bullet+} \quad (1)$$

$$QD+e \rightarrow QD^{\bullet-} \quad (2)$$

$$QD^{\bullet+}+QD^{\bullet-} \rightarrow QD^{*}+QD \quad (3)$$

$$QD^{*} \rightarrow QD+h\nu \quad (4)$$

Examining the relationship between ECL and PL is an effective experimental method to probe the QD surface (Myung et al. 2003, Bae et al. 2004), and thus, the ECL spectrum of PbS QDs was recorded after capping the QDs with TOP ligands. As displayed in Figure 2, the ECL spectrum of PbS QDs demonstrated a maximum wavelength around 910 nm, which was almost identical to that in the PL spectrum of the QDs, indicating that the NIR ECL emission was derived from the original PbS QDs, and the novel NIR ECL emitters, after coating with TOP ligands, had no deep surface traps, causing luminescence at a longer wavelength.

For biological applications, the water-soluble NIR ECL emitters were highly desired. Due to the poor stability of the excited QDs and the limited potential window in the aqueous system, the co-reactant ECL technology

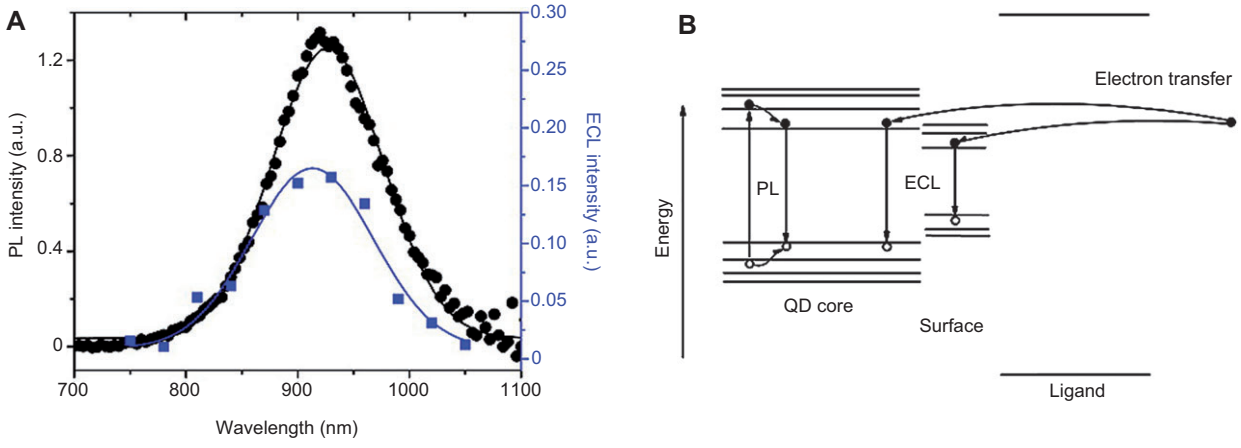

Figure 2 (A) PL (dot) and ECL (square) spectrum of PbS QDs with oleic acid and TOP capping in CH_2Cl_2 containing 0.1 M TBAP. The lines are Gaussian fits to each data set. (B) Schematic mechanism of PL and ECL. (Reproduced with permission from ACS Publication.)

appears as an alternative to the ion annihilation ECL. As the operation of the co-reactant ECL emission features a unidirectional potential scan, this co-reactant-participating ECL course can be further divided into "oxidative-reduction" ECL and "reductive-oxidation" ECL as the different types of electrochemical behaviors toward co-reactants (Miao 2008). The NIR ECL of CdTe QDs has been investigated through the "oxidative-reduction" mechanism using TPrA as a co-reactant (Liang et al. 2011b, Zou et al. 2011). As shown in Eqs. (5)–(8), both CdTe QDs and TPrA were oxidized at the electrode surface and $QD^{\bullet+}$ was reduced by $TPrA^{\bullet}$ to produce the excited state.

$$QD - e \rightarrow QD^{\bullet+} \quad (5)$$

$$TPrA - e \rightarrow TPrA^{\bullet+} \quad (6)$$

$$TPrA^{\bullet+} \rightarrow TPrA^{\bullet} + H^{+} \quad (7)$$

$$QD^{\bullet+} + TPrA^{\bullet} \rightarrow QD^{*} + Pr_2N^{+} \quad (8)$$

By optimizing the reaction conditions including scan rates and pH values, the strong band-gap NIR ECL from this dual-stabilizer-capped CdTe QDs was achieved at a low oxidation potential. This work also gives us a new avenue to overcome two major drawbacks (high emission potential and low ECL intensity) in QD-based ECL systems (Deng and Ju 2013).

Unlike in the above reaction mechanism, "reductive-oxidative" co-reactants can also be used to generate ECL by applying a negative potential. Lately, Pang's group studied the NIR ECL from Ag_2Se QDs produced by the "reductive-oxidation" co-reactant mechanism in an aqueous solution (Cui et al. 2012). In that system, $K_2S_2O_8$ was chosen as the co-reactant, and the light emission processes are given in Eqs. (9)–(13). An electron in the highest occupied molecular orbital (HOMO) of the reduced Ag_2Se QDs was transferred to the strong oxidizing agent ($SO_4^{\bullet-}$) released from the reduction of $S_2O_8^{2-}$, finally leading to an ECL signal. A further comparison between the ECL and PL spectra showed that the ECL peak occurred at the same wavelength as the PL peak, indicating that the surface states of as-prepared Ag_2Se QDs with ultrasmall sizes have been well passivated.

$$S_2O_8^{\bullet+} - e \rightarrow S_2O_8^{\bullet 3-} \quad (9)$$

$$S_2O_8^{\bullet 3-} \rightarrow SO_4^{2-} + SO_4^{\bullet-} \quad (10)$$

$$Ag_2Se + e \rightarrow Ag_2Se^{\bullet} \quad (11)$$

$$Ag_2Se^{\bullet} + SO_4^{\bullet-} \rightarrow Ag_2Se^{*} + SO_4^{2-} \quad (12)$$

$$Ag_2Se^{*} \rightarrow Ag_2Se + h\nu \quad (13)$$

Core/shell structured QDs

To produce a highly improved ECL performance in a QD-based system, especially for NIR ECL, the shell coating for the original emitters is indispensable because the nonradiative dissipation derived from the surface traps can be inhibited effectively by surface passivation. Liang et al. (2010) studied the strong ECL from water-soluble CdSeTe/ZnS QDs and proposed a "reductive-oxidative" co-reactant ECL mechanism. After capping with the ZnS shell, the ECL intensity improved about twice that of CdSeTe QDs. Based on this behavior, our group presented the fabrication of CdTe/CdS/ZnS QDs and the influence of the ZnS shell toward the NIR ECL emitter (Wang et al. 2011). The ZnS shell provided a physical barrier between the emitters (CdTe/CdS) and the surrounding medium, thus increasing the structural stability and protecting the surface properties of the QDs, and further offered an efficient passivation of the surface trap states, giving rise to a strongly enhanced ECL emission. As shown in Figure 3, the CdTe/CdS/ZnS QDs revealed a strong and stable ECL signal at -1.25 V during cathodic scanning, which was nine times greater than the intensity of the maximum ECL emission from CdTe/CdS QDs. The observed similar peaks of the ECL and PL spectra demonstrated that a significant reduction of the deep surface traps from the QDs passivated with the ZnS shell. This work promotes further study on NIR ECL from QDs and impact actively on the development of NIR ECL biosensors.

NIR ECL sensing

By coupling the advantages of both the NIR window and the ECL analytical technique, NIR ECL sensing could probably provide an alternative to both NIR fluorescent bioassay and traditional ECL bioassays, especially in complex biological samples. Based on studies and the far-seeing explorations of the NIR ECL behaviors from QDs, the development of novel NIR ECL sensors from highly luminescent QDs has gained significant progress (Liang et al. 2011b, 2012, Cui et al. 2012, Wang et al. 2012).

NIR ECL for small molecule sensing

The NIR ECL for sensor construction was mainly followed by co-reactant ECL technology, which can be divided into two categories according to the on and off signals on the original ECL signal produced by the

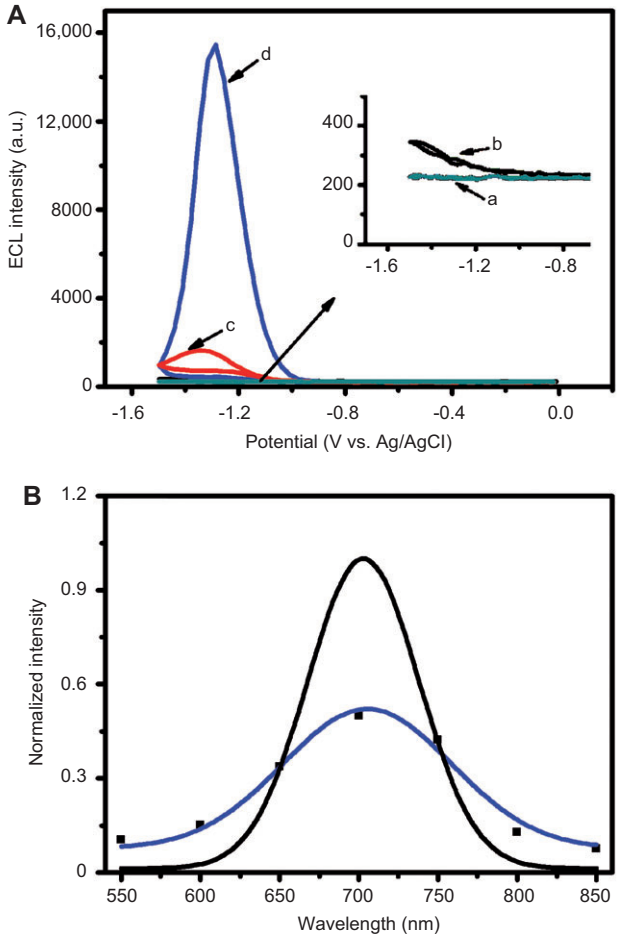

Figure 3 (A) ECL-potential curves of (a) CdTe/CdS/ZnS QDs, (b) 10 mM $K_2S_2O_8$, (c) CdTe/CdS QDs with 10 mM $K_2S_2O_8$, and (d) CdTe/CdS/ZnS QDs with 10 mM $K_2S_2O_8$ in 0.2 M NaAc-HAc buffer solution (pH 7.0). (B) ECL (square) and PL (line) spectra of CdTe/CdS/ZnS QDs.

analyte. Because of the different affinities of sodium hexametaphosphate (HMP) and thiols on the CdTe QD surface, a new NIR ECL strategy for glutathione (L-glutamyl-L-cysteinylglycine, GSH) sensing was developed by Zou's group (Liang et al. 2011b). In their work, the mercaptopropionic acid (MPA)- and HMP-capped CdTe QDs were selected as the NIR ECL emitters. By increasing the concentration ratio of GSH, the GSH molecules could displace the binding sites of the original HMP on the QD surface, making hole injection onto the CdTe surface more difficult and resulting in the decrease of ECL intensity. Under an optimum condition, a wide linear ECL response corresponding to the logarithm concentration of GSH from 50.0 nM to 50.0 μM was obtained with a detection limit of 10.0 nM.

Recently, Pang and colleagues used dopamine (DA) as a model to demonstrate the potential of Ag_2Se QDs in NIR ECL sensors (Cui et al. 2012). They discovered that the cathodic ECL emission produced by Ag_2Se QDs under the assistance of $K_2S_2O_8$ showed a significant decrease after adding DA into the reaction system. This quenching phenomenon was derived from the energy-transfer process from the QDs to DA because the energy level of DA was between the HOMO and the lowest unoccupied molecular orbital of Ag_2Se QDs. A linear relationship ranging from 0.5 to 19 μM was obtained with a detection limit of 0.1 μM. Additionally, the proposed biosensor displayed excellent performance for the detection of the DA concentration in the practical drug.

NIR ECL Immunosensor

The immunoassay, based on highly specific antibody-antigen recognition reactions, has emerged as a powerful sensing tool for the direct detection of disease-related proteins in biological samples. With the increasing demands for early diagnosis of diseases and deep understanding of biological processes in disease evolution, ECL immunoassay has attracted considerable interest because of its intrinsic advantages in terms of high sensitivity, simplified setup, and excellent controllability. The combination of the NIR window and the ECL analytical technique can greatly improve sensitivity due to the efficient decrease of background signals from nontarget biomolecules in the actual sample. Based on the above-mentioned requirements, our group designed and reported a QD-based NIR ECL immunosensor for ultrasensitive human IgG (HIgG) detection using gold nanoparticle-graphene nanosheet (Au-GN) hybrids and SiO_2 nanospheres for dual amplification (Wang et al. 2012). Here, we used the CdTe/CdS $core_{small}$/$shell_{thick}$ QDs as the new NIR ECL emitters because the "thick-shell" model not only largely decreased the surface traps of present QDs but also highly improved their brightness and stability, providing the potential possibility as ECL emitters for NIR sensing as well. As described in Figure 4, integrating the dual amplification from the promoting electron-transfer rate of the Au-GN hybrids and the increasing QD loading of the SiO_2-QD-Ab2 labels, the NIR ECL response from CdTe/CdS QDs enhanced 16.8-fold compared with the unamplified protocol and successfully fulfilled the ultrasensitive detection of HIgG with a detection limit of 87 fg/ml. Moreover, the proposed immunosensor was used to monitor the HIgG level in human serum, and satisfactory results were obtained. This work provided a promising alternative for QD-based NIR PL sensing strategy and intrigued researchers into

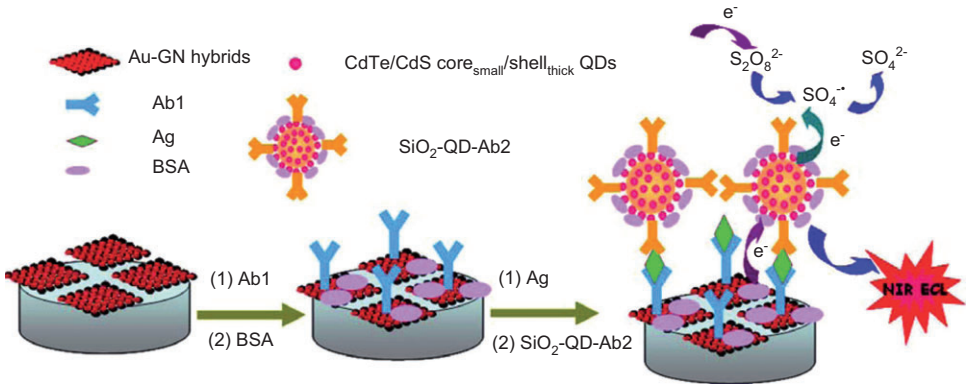

Figure 4 NIR ECL immunoassay of HIgG with dual amplification strategy.

gaining a new interest in the development of NIR ECL immunosensor.

Lately, a sandwich-type NIR ECL immunoassay was developed for α-fetoprotein antigen (AFP) with the dual-stabilizer-capped CdTe QDs as ECL labels (Liang et al. 2012). Because of the advantages of the NIR ECL emission window at 800 nm, low oxidation potential (0.85 V), and high biocompatibility (Figure 5), the proposed immunoassay displayed a good performance toward the AFP with a wide calibration range from 10.0 pg/ml to 80.0 ng/ml and a detection limit of 5.0 pg/ml without coupling any signal amplification procedures. Further, as a practical application, the immunosensor was used to detect the AFP antigen in serum samples with the similar capacity of the $Ru(bpy)_3^{2+}$ reagent kit-based commercial ECL test. They also demonstrated that the difference between the ECL spectrum of the dual-stabilizer-capped CdTe QDs and that of $Ru(bpy)_3^{2+}$ might enable the development of ECL-based multiplexing assay.

Limitations

With the rapidly expanding development of NIR ECL in the field of analytical chemistry, the bioassay of QD-based NIR ECL has four limitations. First, the NIR ECL emissions from the present NIR QDs are relatively weak and unstable, and most need high ECL-triggering potentials (Liang et al. 2010, Wang et al. 2011). Although the surface traps of the dual-stabilizer-capped CdTe QDs can decrease the surface band gap of QD and lead to a low ECL potential, the stability of the proposed biosensors is not very satisfactory due to the drop of capped ligands (Liang et al. 2012). Meanwhile, the shell coating can highly improve the intensity and stability of NIR ECL emission, but the wide band gap tends to generate high electrochemical energies for ECL emission (Liang et al. 2010, Wang et al. 2011, 2012). Therefore, dealing with the relationship among intensity, stability, and potential is the key for the fabrication of QD-based NIR ECL sensors. Second, the detectors of ECL instruments

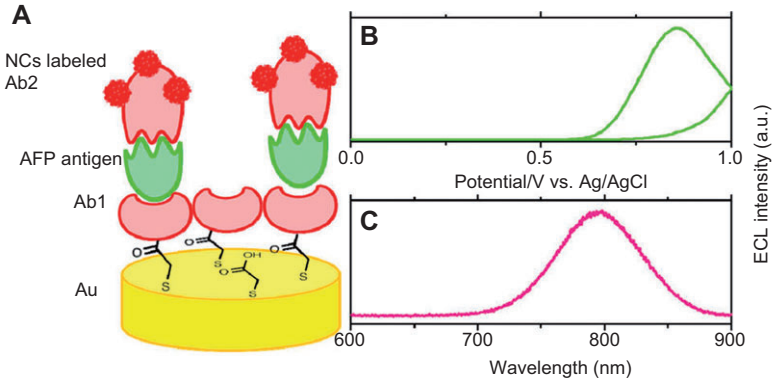

Figure 5 (A) Schematic representation of NIR sandwich-typed immunoassay. (B) ECL-potential curves and (C) ECL spectrum of Au/TGA/Ab1-Ag-Ab2-NCs in 0.10 M pH 9.2 PBS containing 20.0 mM DBAE at a scan rate of 100 mV/s. Ag concentration: 40.0 ng/ml. (Reproduced with permission from ACS Publication.)

toward NIR luminescence were insensitive, especially at a longer wavelength (Wang et al. 2012). The combination of electrochemical workstation with a normal fluorescence instrument may be a smart choice for the signal capture of NIR ECL (Zou et al. 2011). Third, to meet the requirement of completely interference-free sensing in practical applications, there is an urgent demand for exploring and developing new NIR ECL emitters at a longer wavelength (Liang et al. 2012). Fourth, similar to NIR fluorescence sensing, the toxicity of QDs should be taken into account (Cui et al. 2012). It is crucial to pursue studies of cellular sensing for clinical translation. To overcome this hurdle, the NIR ECL of more nontoxic materials such as Ag_2Se QDs needs to be investigated.

Conclusion and outlook

The synthesis, ECL behaviors, and NIR ECL application of NIR QDs have been summarized in this review. NIR ECL analysis could provide an alternative to both the NIR fluorescent bioassay and the traditional ECL bioassays. It is a persistent research motivation to seek novel, efficient QD-based NIR ECL systems (emitters and co-reactants) combined with a deep elucidation of their mechanisms and modern analytical techniques. The significant advantage of interference-free property in complex organism would push forward the development of QD-based NIR ECL imaging.

Acknowledgments: The authors gratefully acknowledge the financial support for this research from the National Natural Science Foundation of China (20975042, 21175051), the Fundamental Research Funds for the Central Universities (2010PY009 and 2010PY139), and the Natural Science Foundation of Hubei Province Innovation Team (2011CDA115).

Received December 29, 2012; accepted March 22, 2013; previously published online April 22, 2013

References

Akamatsu, K.; Tsuruoka, T.; Nawafune, H. Band gap engineering of CdTe nanocrystals through chemical surface modification. *J. Am. Chem. Soc.* **2005**, *127*, 1634–1635.

Allen, P. M.; Bawendi, M. G. Ternary I–III–VI quantum dots luminescent in the red to near-infrared. *J. Am. Chem. Soc.* **2008**, *130*, 9240–9241.

Allen, P. M.; Liu, W.; Chauhan, V. P.; Lee, J.; Ting, A. Y.; Fukumura, D.; Jain, R. K.; Bawendi, M. G. InAs(ZnCdS) quantum dots optimized for biological imaging in the near-infrared. *J. Am. Chem. Soc.* **2009**, *132*, 470–471.

Bae, Y.; Myung, N.; Bard, A. J. Electrochemistry and electrogenerated chemiluminescence of CdTe nanoparticles. *Nano Lett.* **2004**, *4*, 1153–1161.

Bailey, R. E.; Nie, S. Alloyed semiconductor quantum dots: tuning the optical properties without changing the particle size. *J. Am. Chem. Soc.* **2003**, *125*, 7100–7106.

Baker, S. N.; Baker, G. A. Luminescent carbon nanodots: emergent nanolights. *Angew. Chem. Int. Ed.* **2010**, *49*, 6726–6744.

Cai, W.; Shin, D. W.; Chen, K.; Gheysens, O.; Cao, Q.; Wang, S. X.; Gambhir, S. S.; Chen, X. Peptide-labeled near-infrared quantum dots for imaging tumor vasculature in living subjects. *Nano Lett.* **2006**, *6*, 669–676.

Chen, C.-Y.; Cheng, C.-T.; Yu, J.-K.; Pu, S.-C.; Cheng, Y.-M.; Chou, P.-T. Spectroscopy and femtosecond dynamics of type-II CdSe/ZnTe core-shell semiconductor synthesized via the CdO precursor. *J. Phys. Chem. B* **2004**, *108*, 10687–10691.

Chen, L. N.; Wang, J.; Li, W. T.; Han, H. Y. Aqueous one-pot synthesis of bright and ultrasmall CdTe/CdS near-infrared-emitting quantum dots and their application for tumor targeting *in vivo*. *Chem. Commun*. **2012**, *48*, 4971.

Choi, H. S.; Ipe, B. I.; Misra, P.; Lee, J. H.; Bawendi, M. G.; Frangioni, J. V. Tissue- and organ-selective biodistribution of NIR fluorescent quantum dots. *Nano Lett.* **2009**, *9*, 2354–2359.

Cui, R.; Gu, Y. P.; Bao, L.; Zhao, J. Y.; Qi, B. P.; Zhang, Z. L.; Xie, Z. X.; Pang, D. W. Near-infrared electrogenerated chemiluminescence of ultrasmall Ag_2Se quantum dots for the detection of dopamine. *Anal. Chem.* **2012**, *84*, 8932–8935.

Deng, S.; Ju, H. Electrogenerated chemiluminescence of nanomaterials for bioanalysis. *Analyst* **2013**, *138,* 43.

Deng, Z.; Schulz, O.; Lin, S.; Ding, B.; Liu, X.; Wei, X.; Ros, R.; Yan, H.; Liu, Y. Aqueous synthesis of zinc blende CdTe/CdS magic-core/thick-shell tetrahedral-shaped nanocrystals with emission tunable to near-infrared. *J. Am. Chem. Soc.* **2010**, *132*, 5592–5593.

Dennany, L.; Forster, R. J.; Rusling, J. F. Simultaneous direct electrochemiluminescence and catalytic voltammetry detection of DNA in ultrathin films. *J. Am. Chem. Soc.* **2003**, *125*, 5213–5218.

Dennany, L.; O'Reilly, E. J.; Keyes, T. E.; Forster, R. J. Electrochemiluminescent monolayers on metal oxide electrodes: detection of amino acids. *Electrochem. Commun*. **2006**, *8*, 1588–1594.

Díez, I.; Pusa, M.; Kulmala, S.; Jiang, H.; Walther, A.; Goldmann, A. S.; Müller, A. H. E.; Ikkala, O.; Ras, R. H. A. Color tunability and electrochemiluminescence of silver nanoclusters. *Angew. Chem. Int. Ed.* **2009**, *48*, 2122–2125.

Ding, Z.; Quinn, B.; Haram, S.; Pell, L.; Korgel, B.; Bard, A. Electrochemistry and electrogenerated chemiluminescence from silicon nanocrystal quantum dots. *Science* **2002**, *296*, 1293–1297.

Du, Y.; Xu, B.; Fu, T.; Cai, M.; Li, F.; Zhang, Y.; Wang, Q. Near-infrared photoluminescent Ag_2S quantum dots from a single source precursor. *J. Am. Chem. Soc.* **2010**, *132*, 1470–1471.

Erogbogbo, F.; Yong, K.; Roy, I.; Xu, G.; Prasad, P.; Swihart. M. Biocompatible luminescent silicon quantum dots for imaging of cancer cells. *ACS Nano* **2008**, *2*, 873–878.

Evans, C. M.; Guo, L.; Peterson, J. J.; Maccagnano-Zacher, S.; Krauss, T. D. Ultrabright PbSe magic-sized clusters. *Nano Lett*. **2008**, *8*, 2896–2899.

Frangioni, J. In vivo near-infrared fluorescence imaging. *Curr. Opin. Chem. Biol*. **2003**, *7*, 626–634.

Gao, J.; Chen, K.; Xie, R.; Xie, J.; Lee, S.; Cheng, Z.; Peng, X.; Chen, X. Ultrasmall near-infrared non-cadmium quantum dots for in vivo tumor imaging. *Small* **2010**, *6*, 256–261.

Green, M.; Wakefield, G.; Dobson, P. J. A simple metalorganic route to organically passivated mercury telluride nanocrystals. *J. Mater. Chem*. **2003**, *13*, 1076–1078.

Gu, Y.; Cui, R.; Zhang, Z.; Xie, Z.; Pang, D. Ultrasmall near-infrared Ag_2Se quantum dots with tunable fluorescence for *in vivo* imaging. *J. Am. Chem. Soc.* **2012**, *134*, 79–82.

Guzelian, A. A.; Katari, J. E. B.; Kadavanich, A. V.; Banin, U.; Hamad, K.; Juban, E.; Alivisatos, A. P.; Wolters, R. H.; Arnold, C. C.; Heath, J. R. Synthesis of size-selected, surface-passivated InP nanocrystals. *J. Phys. Chem*. **1996**, *100*, 7212–7219.

Han, H.; Sheng, Z.; Liang, J. Electrogenerated chemiluminescence from thiol-capped CdTe quantum dots and its sensing application in aqueous solution. *Anal. Chim. Acta* **2007**, *596*, 73–78.

Haubold, S.; Haase, M.; Kornowski, A.; Weller, H. Strongly luminescent InP/ZnS core-shell nanoparticles. *ChemPhysChem* **2001**, *2*, 331–334.

He, Y.; Zhong, Y.; Su, Y.; Lu, Y.; Jiang, Z.; Peng, F.; Xu, T.; Su, S.; Huang, Q.; Fan, C.; Lee, S. T. Water-dispersed near-infrared-emitting quantum dots of ultrasmall sizes for *in vitro* and *in vivo* imaging. *Angew. Chem. Int. Ed*. **2011a**, *50*, 5695–5698.

He, Y.; Zhong, Y.; Peng, F.; Wei, X.; Su, Y.; Lu, Y.; Su, S.; Gu, W.; Liao, L.; Lee. S. One-pot microwave synthesis of water-dispersible, ultraphoto- and pH-stable, and highly fluorescent silicon quantum dots. *J. Am. Chem. Soc.* **2011b**, *133*, 14192–14195.

Higginson, K. A.; Kuno, M.; Bonevich, J.; Qadri, S. B.; Yousuf, M.; Mattoussi, H. Synthesis and characterization of colloidal β-HgS quantum dots. *J. Phys. Chem. B* **2002**, *106*, 9982–9985.

Hinds, S.; Myrskog, S.; Levina, L.; Koleilat, G.; Yang, J.; Kelley, S. O.; Sargent, E. H. NIR-emitting colloidal quantum dots having 26% luminescence quantum yield in buffer solution. *J. Am. Chem. Soc.* **2007**, *129*, 7218–7219.

Hu, L.; Xu, G. Applications and trends in electrochemiluminescence. *Chem. Soc. Rev*. **2010**, *39*, 3275–3304.

Hu, X.; Han, H.; Hua, L.; Sheng, Z. Electrogenerated chemiluminescence of blue emitting ZnSe quantum dots and its biosensing for hydrogen peroxide. *Biosens. Bioelectron*. **2010**, *25*, 1843–1846.

Jiang, P.; Tian, Z.; Zhu, C.; Zhang, Z.; Pang, D. Emission-tunable near-infrared Ag_2S quantum dots. *Chem. Mater.* **2012**, *24*, 3–5.

Jie, G. F.; Liu, B.; Pan, H. C.; Zhu, J. J.; Chen, H. Y. CdS nanocrystal-based electrochemiluminescence biosensor for the detection of low-density lipoprotein by increasing sensitivity with gold nanoparticle amplification. *Anal. Chem*. **2007**, *79*, 5574–5581.

Kim, S.; Fisher, B.; Eisler, H. J.; Bawendi, M. Type-II quantum dots: CdTe/CdSe (core/shell) and CdSe/ZnTe (core/shell) heterostructures. *J. Am. Chem. Soc.* **2003a**, *125*, 11466–11467.

Kim, S.; Lim, Y. T.; Soltesz, E. G.; De Grand, A. M.; Lee, J.; Nakayama, A.; Parker, J. A.; Mihaljevic, T.; Laurence, R. G.; Dor, D. M.; Cohn, L. H.; Bawendi, M. G.; Frangioni, J. V. Near-infrared fluorescent type II quantum dots for sentinel lymph node mapping. *Nat. Biotechnol*. **2003b**, *22*, 93–97.

Li, L.; Protière, M.; Reiss, P. Economic synthesis of high quality InP nanocrystals using calcium phosphide as the phosphorus precursor. *Chem. Mater*. **2008**, *20*, 2621–2623.

Li, L.; Liu, H.; Shen, Y.; Zhang, J.; Zhu, J. J. Electrogenerated chemiluminescence of Au nanoclusters for the detection of dopamine. *Anal. Chem*. **2011**, *83*, 661–665.

Li, J.; Guo, S.; Wang, E. Recent advances in new luminescent nanomaterials for electrochemiluminescence sensors. *RSC Adv.* **2012**, *2*, 3579.

Liang, G. X.; Gu, M. M.; Zhang, J. R.; Zhu, J. J. Preparation and bioapplication of high-quality, water-soluble, biocompatible, and near-infrared-emitting CdSeTe alloyed quantum dots. *Nanotechnology* **2009**, *20*, 415103–415112.

Liang, G. X.; Li, L. L.; Liu, H. Y.; Zhang, J. R.; Burda, C.; Zhu, J. J. Fabrication of near-infrared-emitting CdSeTe/ZnS core/shell quantum dots and their electrogenerated chemiluminescence. *Chem. Commun*. **2010**, *46*, 2974–2977.

Liang, G.; Shen, L.; Zhang, X.; Zou, G. One-pot synthesis of dual-stabilizer-capped CdTe nanocrystals with efficient near-infrared photoluminescence and electrochemiluminescence. *Eur. J. Inorg. Chem*. **2011a**, *25*, 3726–3730.

Liang, G.; Shen, L.; Zou, G.; Zhang, X. Efficient near-infrared electrochemiluminescence from CdTe nanocrystals with low triggering potential and ultrasensitive sensing ability. *Chem. Eur. J*. **2011b**, *17*, 10213–10215.

Liang, G.; Liu, S.; Zou, G.; Zhang, X. Ultrasensitive immunoassay based on anodic near-infrared electrochemiluminescence from dual-stabilizer-capped CdTe nanocrystals. *Anal. Chem*. **2012**, *84*, 10645–10649.

Ma, Q.; Su, X. Near-infrared quantum dots: synthesis, functionalization and analytical applications. *Analyst* **2010**, *135*, 1867–1877.

Mao, W.; Guo, J.; Yang, W.; Wang, C.; He, J.; Chen, J. Synthesis of high-quality near-infrared-emitting CdTeS alloyed quantum dots via the hydrothermal method. *Nanotechnology* **2007**, *18*, 485611.

Miao, W. Electrogenerated chemiluminescence and its biorelated applications. *Chem. Rev*. **2008**, *108*, 2506–2553.

Miao, W.; Choi, J. P.; Bard, A. J. Electrogenerated Chemiluminescence 69: The Tris(2,2′-bipyridine)ruthenium(II), $(Ru(bpy)_3^{2+})$/Tri-n-propylamine (TPrA) system revisited – a new route involving $TPrA^{\cdot+}$ cation radicals. *J. Am. Chem. Soc.* **2002**, *124*, 14478–14485.

Mićić, O. I.; Cheong, H. M.; Fu, H.; Zunger, A.; Sprague, J. R.; Mascarenhas, A.; Nozik, A. J. Size-dependent spectroscopy of InP quantum dots. *J. Phys. Chem. B* **1997**, *101*, 4904–4912.

Mićić, O. I.; Smith, B. B.; Nozik, A. J. Core-shell quantum dots of lattice-matched $ZnCdSe_2$ shells on InP cores: experiment and theory. *J. Phys. Chem. B* **2000**, *104*, 12149–12156.

Mokkapati, S.; Jagadish, C. III–V compound SC for optoelectronic devices. *Mater. Today* **2009**, *12*, 22–32.

Myung, N.; Ding, Z.; Bard, A. J. Electrogenerated chemiluminescence of CdSe nanocrystals. *Nano Lett*. **2002**, *2*, 1315–1319.

Myung, N.; Bae, Y.; Bard, A. J. Effect of surface passivation on the electrogenerated chemiluminescence of CdSe/ZnSe nanocrystals. *Nano Lett*. **2003**, *3*, 1053–1055.

Peng, Z. A.; Peng, X. Formation of high-quality CdTe, CdSe, and CdS nanocrystals using CdO as precursor. *J. Am. Chem. Soc.* **2000**, *123*, 183–184.

Qi, H.; Peng, Y.; Gao, Q.; Zhang, C. Applications of nanomaterials in electrogenerated chemiluminescence biosensors. *Sensors* **2009**, *9*, 674–695.

Reiss, P.; Protière, M.; Li, L. Core/shell semiconductor nanocrystals. *Small* **2009**, *5*, 154–168.

Richter, M. M. Electrochemiluminescence (ECL). *Chem. Rev.* **2004**, *104*, 3003–3036.

Smith, A. M.; Mohs, A. M.; Nie, S. Tuning the optical and electronic properties of colloidal nanocrystals by lattice strain. *Nat. Nanotechnol.* **2008**, *4*, 56–63.

Sun, L.; Bao, L.; Hyun, B. R.; Bartnik, A. C.; Zhong, Y. W.; Reed, J. C.; Pang, D. W.; Abruña, H. C. D.; Malliaras, G. G.; Wise, F. W. Electrogenerated chemiluminescence from PbS quantum dots. *Nano Lett.* **2009**, *9*, 789–793.

Talapin, D. V.; Haubold, S.; Rogach, A. L.; Kornowski, A.; Haase, M.; Weller, H. A novel organometallic synthesis of highly luminescent CdTe nanocrystals. *J. Phys. Chem. B* **2001**, *105*, 2260–2263.

Talapin, D. V.; Gaponik, N.; Borchert, H.; Rogach, A. L.; Haase, M.; Weller, H. Etching of colloidal InP nanocrystals with fluorides: photochemical nature of the process resulting in high photoluminescence efficiency. *J. Phys. Chem. B* **2002**, *106* 12659–12663.

Tian, D.; Duan, C.; Wang, W.; Cui, H. Ultrasensitive electrochemiluminescence immunosensor based on luminol functionalized gold nanoparticle labeling. *Biosens. Bioelectron.* **2010**, *25*, 2290–2295.

Wang, J.; Han, H. Hydrothermal synthesis of high-quality type-II CdTe/CdSe quantum dots with near-infrared fluorescence. *J. Colloid Interf. Sci.* **2010**, *351*, 83–87.

Wang, J.; Jiang, X.; Han, H.; Li, N. Cathodic electrochemiluminescence from self-designed near-infrared-emitting CdTe/CdS/ZnS quantum dots on bare Au electrode. *Electrochem. Commun.* **2011**, *13*, 359–362.

Wang, J.; Han, H.; Jiang, X.; Huang, L.; Chen, L.; Li, N. Quantum dot-based near-infrared electrochemiluminescent immunosensor with gold nanoparticle-graphene nanosheet hybrids and silica nanospheres double-assisted signal amplification. *Anal. Chem.* **2012**, *84*, 4893–4899.

Wilson, R.; Clavering, C.; Hutchinson, A. Electrochemiluminescence enzyme immunoassays for TNT and pentaerythritol tetranitrate. *Anal. Chem.* **2003**, *75*, 4244–4249.

Xie, R.; Peng, X. Synthetic scheme for high-quality InAs nanocrystals based on self-focusing and one-pot synthesis of InAs-based core-shell nanocrystals. *Angew. Chem. Int. Ed.* **2008**, *120*, 7677–7680.

Xie, R.; Peng, X. Synthesis of Cu-doped InP nanocrystals (d-dots) with ZnSe diffusion barrier as efficient and color-tunable NIR emitters. *J. Am. Chem. Soc.* **2009**, *131*, 10645–10651.

Xie, R.; Zhong, X.; Basché, T. Synthesis, characterization, and spectroscopy of type-II core/shell semiconductor nanocrystals with ZnTe cores. *Adv. Mater.* **2005**, *17*, 2741–2745.

Xie, R.; Battaglia, D.; Peng, X. Colloidal InP nanocrystals as efficient emitters covering blue to near-infrared. *J. Am. Chem. Soc.* **2007**, *129*, 15432–15433.

Yong, K. T.; Roy, I.; Ding, H.; Bergey, E. J.; Prasad, P. N. Biocompatible near-infrared quantum dots as ultrasensitive probes for long-term *in vivo* imaging applications. *Small* **2009**, *5*, 1997–2004.

Zhan, W.; Bard, A. J. Electrogenerated chemiluminescence. 83. immunoassay of human C-reactive protein by using $Ru(bpy)_3^{2+}$-encapsulated liposomes as labels. *Anal. Chem.* **2006**, *79*, 459–463.

Zhang, Z. F.; Cui, H.; Lai, C. Z.; Liu, L. J. Gold nanoparticle-catalyzed luminol chemiluminescence and its analytical applications. *Anal. Chem.* **2005**, *77*, 3324–3329.

Zhang, Y.; Li, Y.; Yan, X. P. Aqueous layer-by-layer epitaxy of type-II CdTe/CdSe quantum dots with near-infrared fluorescence for bioimaging applications. *Small* **2009**, *5*, 185–189.

Zhang, Y.; Hong, G.; Zhang, Y.; Chen, G.; Li, F.; Dai, H.; Wang, Q. Ag_2S quantum dot: a bright and biocompatible fluorescent nanoprobe in the second near-infrared window. *ACS Nano* **2012**, *6*, 3695–3702.

Zheng, L. Y.; Chi, Y. W.; Dong, Y. Q.; Lin, J. P.; Wang, B. B. Electrochemiluminescence of water-soluble carbon nanocrystals released electrochemically from graphite. *J. Am. Chem. Soc.* **2009**, *131*, 4564–4565.

Zhu, C.; Jiang, P.; Zhang, Z.; Zhu, D.; Tian, Z.; Pang, D. Ag_2Se quantum dots with tunable emission in the second near-infrared window. *ACS Appl. Mater. Interfaces* **2013**, *5*, 1186–1189.

Zou, G.; Ju, H. Electrogenerated chemiluminescence from a CdSe nanocrystal film and its sensing application in aqueous solution. *Anal. Chem.* **2004**, *76*, 6871–6876.

Zou, L.; Gu, Z.; Zhang, N.; Zhang, Y.; Fang, Z.; Zhu, W.; Zhong, X. Ultrafast synthesis of highly luminescent green- to near infrared-emitting CdTe nanocrystals in aqueous phase. *J. Mater. Chem.* **2008**, *18*, 2807–2815.

Zou, G.; Liang, G.; Zhang, X. Strong anodic near-infrared electrochemiluminescence from CdTe quantum dots at low oxidation potentials. *Chem.Commun.* **2011**, *47*, 10115–10118.

Zu, Y.; Bard, A. J. Electrogenerated chemiluminescence. 66. the role of direct coreactant oxidation in the ruthenium tris(2,2′) bipyridyl/tripropylamine system and the effect of halide ions on the emission intensity. *Anal. Chem.* **2000**, *72*, 3223–3232.

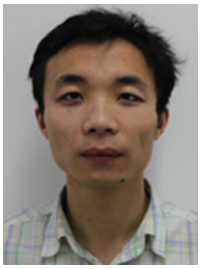

Jing Wang was born in Zhejiang Province, China, in 1986. He received his BS degree in 2008, and he is currently a PhD student in Huazhong Agricultural University under the direction of Professor Heyou Han. His scientific interests are focused on functionalized quantum dots for fluorescent and electrochemiluminescent applications.

Heyou Han was born in Anhui Province, China, in 1962. He received his PhD degree from Wuhan University in 2000, and he worked on his postdoctoral research in Jackson State University (Jackson, MS, USA) from 2000 to 2004. He has been a Professor at Huazhong Agricultural University since 2004. He has published more than 80 papers in international journals. His research interests are focused on functionalized nanomaterials for bioanalytical, food safety, and energy applications.